

Preparation and photoluminescence properties of $\text{LaGaO}_3:0.05\text{Tb}^{3+}$ green phosphors

ZHAO LI*, YUN-ZHENG WANG, HONG-BO JI, KUN-YAO WU

School of Materials Engineering, Xi'an Aeronautical University, Xi'an 710077, China

$\text{LaGaO}_3:0.05\text{Tb}^{3+}$ green phosphors were prepared via high-temperature solid-phase calcination at a temperature of 1300 °C for 4 h in a reducing environment. The crystalline structure, microscopic morphology and luminescence of the phosphor samples were characterized using X-ray diffractometer (XRD), scanning electron microscope (SEM) and fluorescence spectrometer (PL), respectively, alongside a deployment of color coordinate calculation software (CIE). The results showed that the $\text{LaGaO}_3:0.05\text{Tb}^{3+}$ green phosphors were pure in terms of phase composition and had complete crystalline structure with regular morphology and uniform particle distribution. The photoluminescence process involved the $4f \rightarrow 5d \rightarrow 4f$ energy level transition of Tb^{3+} , in which the excitation peak was located at 378 nm and the emission peak was found at 545 nm. The color coordinate of the $\text{LaGaO}_3:0.05\text{Tb}^{3+}$ phosphor was determined as (0.3481, 0.4228), which corresponded to the emission of relatively pure green light. Finally, the self-made $\text{LaGaO}_3:0.05\text{Tb}^{3+}$ green phosphors along with commercially available red and blue phosphors were employed as the raw materials for assembling a LED device, which exhibited excellent white light emission performance.

(Received September 22, 2022; accepted November 24, 2023)

Keywords: $\text{LaGaO}_3:0.05\text{Tb}^{3+}$, Green phosphors, WLED, Luminescence

1. Introduction

White light producing LEDs are commonly known as fourth-generation lighting sources due to their advantages of high luminous efficiency, low power consumption, long service life, and zero environmental impact[1-3]. At present, there are three main ways to create white light LEDs[4]. The first is the combination of LED chips that emit blue light with yellow light emitting phosphor materials. The latter are effectively excited by blue light to form white LEDs (WLEDs). Meanwhile, in spite of simplicity and maturity, this technology possesses shortcomings such as the lack of red light and poor color rendering. The second possibility is a combination of blue, green, and red chips. The white light (as perceived by the naked eye) arises when these three primary colors mix together, after which a current can be applied to the chips. However, the structure is complex and requires numerous chips, thereby increasing the manufacturing cost and hindering the mass production of such a device. The third method is the combination of blue, green, and red phosphors that are excited by near-ultraviolet or blue light. Here, the rare earth ions present in the phosphors absorb the electromagnetic radiation energy and undergo energy level transitions that result in the irradiation of blue, green and red light whose superposition yields the visible white light. This method provides efficient white light color rendering and high stability at a low cost, which make it ideal for obtaining powerful white light LEDs for a wide range of applications.

Among the primary color phosphors, the red and the blue phosphors are already relatively mature. Therefore, this work aims to investigate the green phosphors. More precisely, a series of LaGaO_3 green phosphors were examined. LaGaO_3 green phosphors have recently received extensive attention and are increasingly used as a new type of luminescent materials[5-6]. In particular, Liu Xiaoming et al.[7] prepared Tb^{3+} -doped LaGaO_3 phosphors through a Pechini-type sol-gel process. And the XRD results revealed that the sample began to crystallize at 900 °C and a pure LaGaO_3 phase could be obtained at 1000 °C. The FESEM images indicated that the Tb^{3+} -doped LaGaO_3 phosphors were composed of aggregated spherical particles with sizes ranging from 40 to 80 nm. $\text{LaGaO}_3:\text{Tb}^{3+}$ and $\text{LaGaO}_3:(\text{Tb}^{3+},\text{Li}^+/\text{Na}^+/\text{K}^+)$ phosphors were produced via a high-temperature solid-phase synthesis method using La_2O_3 , Ga_2O_3 , Tb_4O_7 , Li_2CO_3 , Na_2CO_3 , and K_2CO_3 as the raw materials. The properties of the phosphors were then analyzed by various experimental means.

2. Preparation and characterization of materials

2.1. Preparation process

$\text{LaGaO}_3:\text{Tb}^{3+}$ and $\text{LaGaO}_3:(\text{Tb}^{3+},\text{Li}^+/\text{Na}^+/\text{K}^+)$ green phosphors co-doped with different concentrations of Li^+ , Na^+ , and K^+ were prepared by a high-temperature solid-

phase synthesis method according to the following steps. First, La_2O_3 , Ga_2O_3 , Tb_4O_7 , Li_2CO_3 , Na_2CO_3 and K_2CO_3 were accurately weighed and thoroughly ground in an agate mortar for 40 min after the dropwise addition of anhydrous ethanol. The as-obtained precursors of the $\text{LaGaO}_3:(\text{Tb}^{3+}, \text{Li}^+/\text{Na}^+/\text{K}^+)$ green phosphors were then reduced in a muffle furnace. The target products were acquired by calcination at a temperature of 1300 °C for 4 h. Commercial blue phosphors BAM and $(\text{Ca}, \text{Sr})\text{AlSiN}_3:\text{Eu}^{2+}$ red phosphors were afterward added to the $\text{LaGaO}_3:\text{Tb}^{3+}$ green phosphors with respect to a ratio of 7.5:2:1 for the green, blue, and red phosphors, respectively. ZWL8820 organic gel was also used. The mass ratio of the silica powder was 1:1.2 for the mixing process.

2.2. Analytical characterization

The crystalline structure of the $\text{LaGaO}_3:\text{Tb}^{3+}$ green phosphor was determined by employing a Rigaku Ultima IV X-ray diffractometer (Rigaku Corp., Japan). The apparent morphology was examined by using a Zeiss Sigma 300 field emission scanning electron microscope (Bruker, Germany). The excitation and emission spectra of the phosphors were excited by an FLS1000 fluorescence spectrometer (Edinburgh). The chromaticity coordinates and the color rendering indices of the LED devices were measured by means of a Hongpu HP9000 LED device

testing system. All the tests were implemented at room temperature.

3. Results and discussion

3.1. Phase structure analysis

Fig. 1 shows the X-ray diffraction patterns of $\text{LaGaO}_3:0.05\text{Tb}^{3+}$ and $\text{LaGaO}_3:(0.05\text{Tb}^{3+}, \text{Li}^+/\text{Na}^+/\text{K}^+)$ green phosphors. The data acquired from $\text{LaGaO}_3:\text{Tb}^{3+}$ matched well with a relevant standard PDF card (PDF#24-1102), revealing no impurity-related peaks. Since the radius of Tb^{3+} ion (0.0923 nm) is smaller than that of La^{3+} (0.1032 nm), the results indicated that Tb^{3+} ions were successfully embedded in the LaGaO_3 matrix, replacing La atoms without modifying the phase structure. Simultaneously, the introduction of trace amounts of Li^+ , Na^+ , and K^+ had no effect on the structure of the lanthanum gallate phosphors. This is because the ions could be easily incorporated into the crystalline matrix without changing its structure. However, after alkali metal doping, the intensities of XRD peaks of the product were enhanced but their positions remained unchanged, mainly due to the fact that doping reduced the crystal defect concentration, thereby increasing the crystallization degree of the sample.

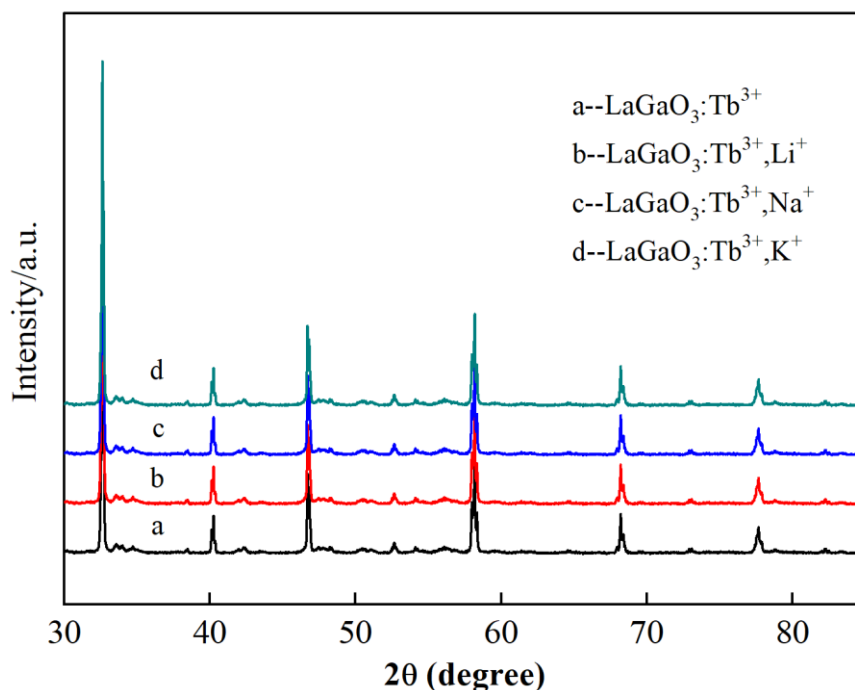


Fig. 1. XRD patterns of $\text{LaGaO}_3:0.05\text{Tb}^{3+}$ and $\text{LaGaO}_3:(0.05\text{Tb}^{3+}, \text{Li}^+/\text{Na}^+/\text{K}^+)$ phosphors (color online)

3.2. Micro-morphology and energy spectrum analysis

Fig. 2 displays the scanning electron microscope micrographs of $\text{LaGaO}_3:\text{Tb}^{3+}$ phosphors at different

magnifications. It can be seen from Fig. 2 that the $\text{LaGaO}_3:\text{Tb}^{3+}$ phosphor samples prepared via the high-temperature solid-phase method had good dispersibility. In addition, the microscopic morphology was presented by spherical particle agglomerates in which the particle size

was around 1 μm . It is noteworthy that the particle size, morphology and dispersibility can affect the luminous flux, light decay, encapsulation coating and other properties of the phosphor powder. A too large particle size

leads to an uneven coating of the phosphor powder, whereas too small particles reduce the UV light absorption, which increases the ultraviolet radiation and decreases the luminous efficiency of the phosphor[8,9].

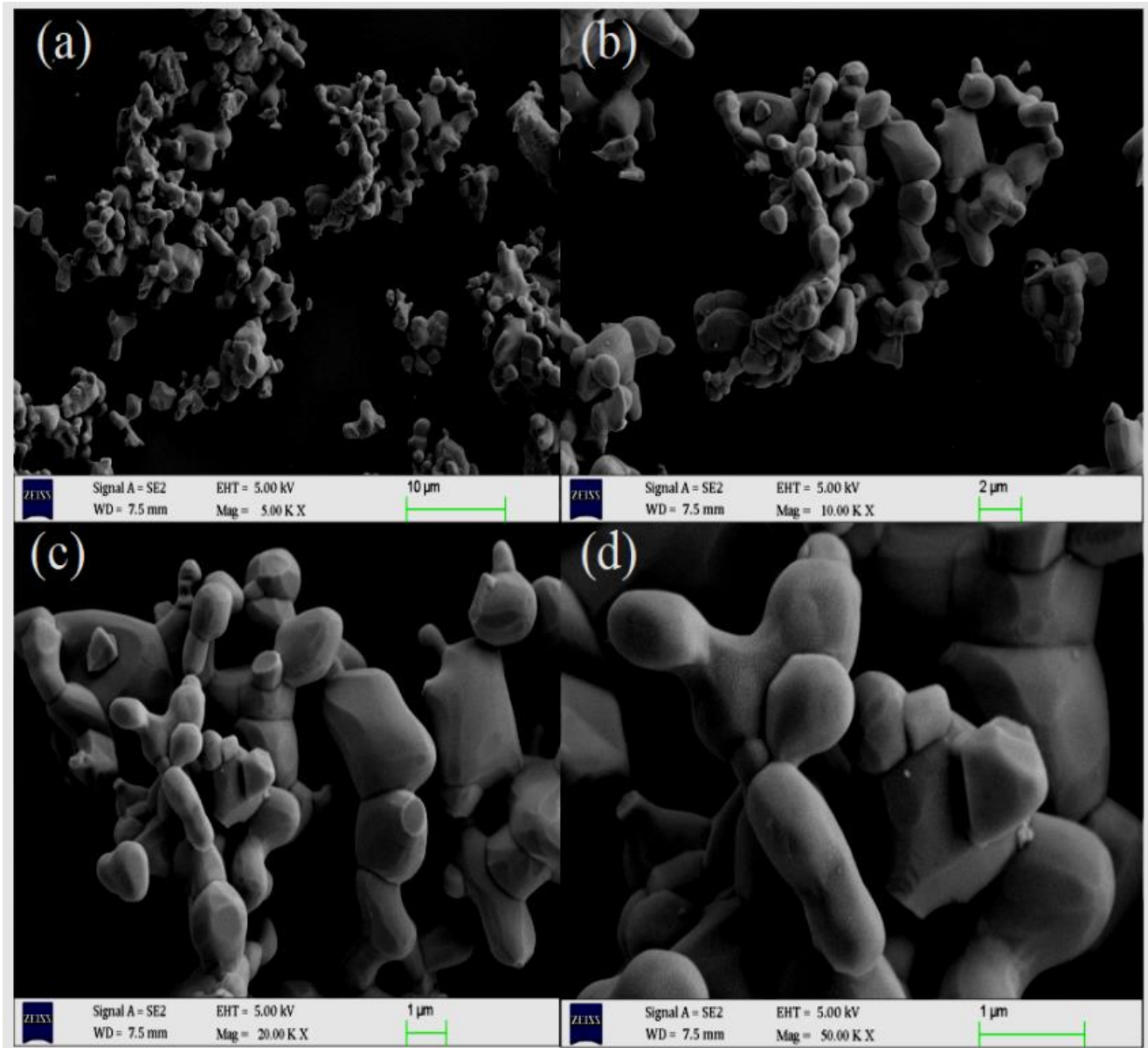


Fig. 2. SEM images of the $\text{LaGaO}_3:\text{Tb}^{3+}$ phosphor (color online)

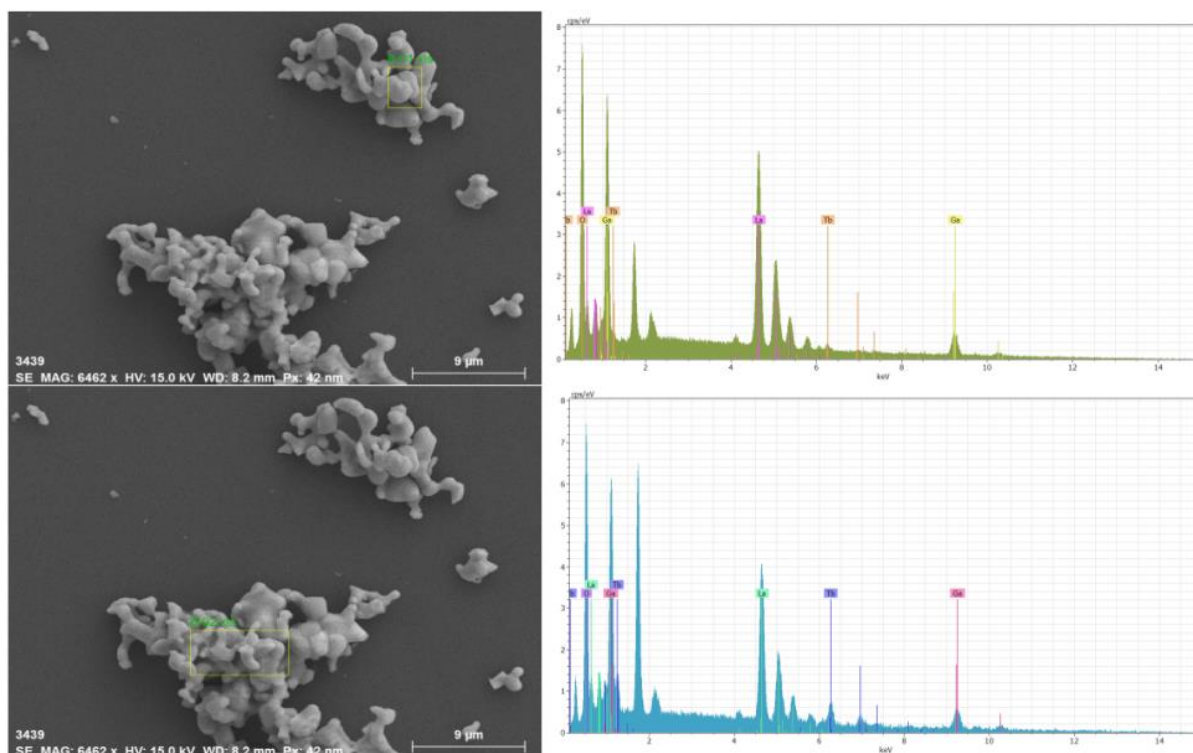


Fig. 3. Spot scan energy spectra of the $\text{LaGaO}_3:\text{Tb}^{3+}$ phosphor (color online)

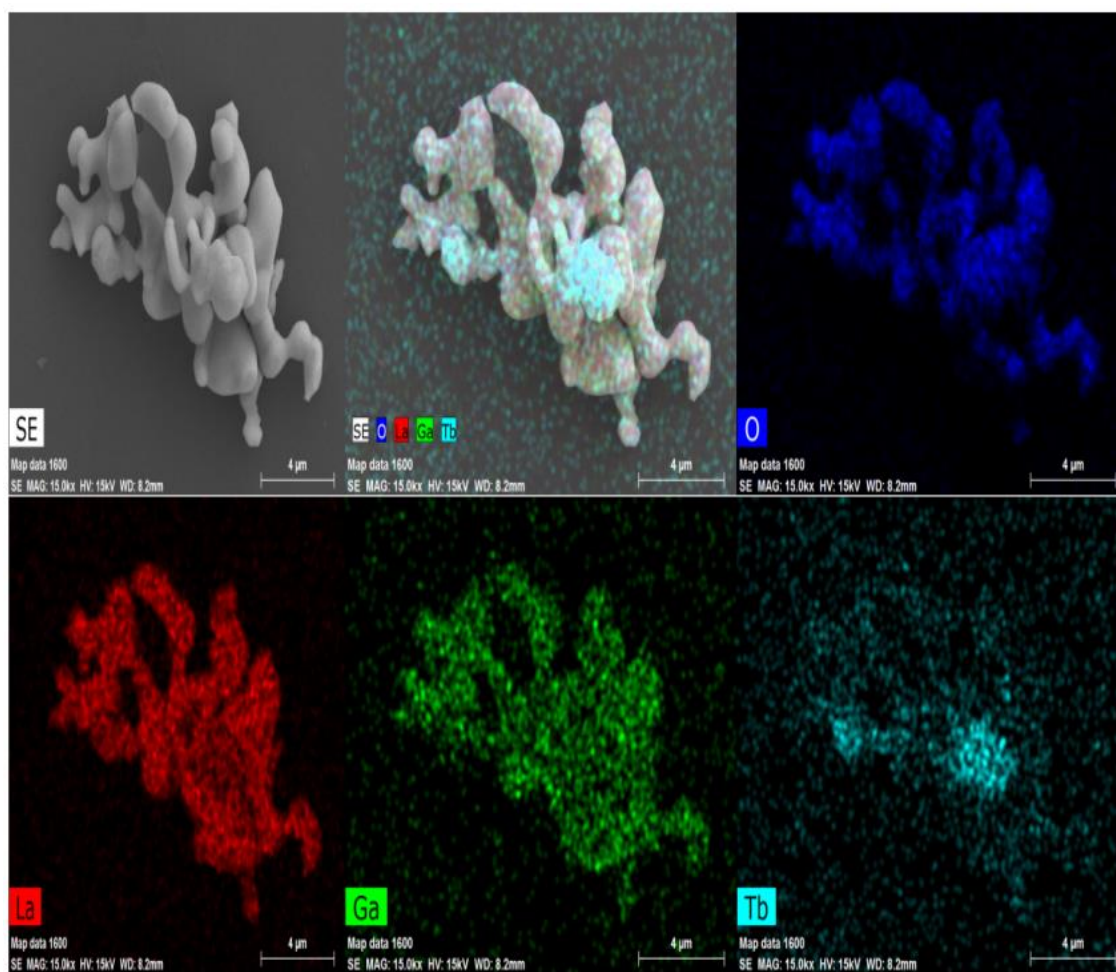


Fig. 4. EDS maps of the $\text{LaGaO}_3:\text{Tb}^{3+}$ phosphor (color online)

Two different points at the surface of $\text{LaGaO}_3:\text{Tb}^{3+}$ phosphor were arbitrarily selected for the EDS analysis, and the results are shown in Fig. 3, revealing the expected elemental contents within the $\text{LaGaO}_3:\text{Tb}^{3+}$ and $\text{LaGaO}_3:(\text{Tb}^{3+},\text{Li}^+)$ phosphors. Fig. 4 depicts the EDS surface scans of the $\text{LaGaO}_3:\text{Tb}^{3+}$ phosphor powder, in which the blue, red, green and light blue colors represent oxygen, lanthanum, gallium and terbium elements, respectively. It is clear that the element composition is consistent with the point scan results, and the distribution of each element is uniform. Therefore, the XRD and EDS data confirmed that the Tb^{4+} ions were successfully introduced into the LaGaO_3 matrix by replacing La, and no phase impurities occurred.

3.3. Excitation and emission spectroscopy analysis

The excitation spectrum of the $\text{LaGaO}_3:0.05\text{Tb}^{3+}$ phosphor is shown in Fig. 5, in which the main excitation peak at a wavelength of 378 nm is assigned to the ultraviolet light range. Therefore, it can be concluded that the $\text{LaGaO}_3:\text{Tb}^{3+}$ green phosphor can be effectively excited by ultraviolet light, which corresponds to the $4f \rightarrow 5d \rightarrow 4f$ energy level transition for the valence electrons of the Tb^{3+} ion, resulting in a large number of luminescent centers. In summary, the excitation spectrum of the sample consisted of sharp peaks at 300–500 nm, which were attributed to the f-f characteristic excitation transitions of Tb^{3+} ions, such as $^7\text{F}_6 \rightarrow ^5\text{H}_6$, $^5\text{H}_7$, $^5\text{L}_6$, $^5\text{L}_9$, $^5\text{L}_{10}$, $^5\text{G}_9$, and $^5\text{D}_4$.

The emission spectrum of the $\text{LaGaO}_3:0.05\text{Tb}^{3+}$ phosphor was excited by ultraviolet light with a wavelength of 378 nm, and the results are shown in Fig. 6. The strongest emission from the $\text{LaGaO}_3:0.05\text{Tb}^{3+}$ phosphor is observed at 545 nm. Fig. 7 depicts the emission spectrum of the $\text{LaGaO}_3:0.05\text{Tb}^{3+}$ phosphor doped with the alkali metal ions. Herein, the doping with Li^+ , Na^+ and K^+ ions is shown to improve the luminescence intensity of the sample. Hence, the co-doping with alkali metal ions is found to be beneficial for the luminous emission intensity of the lanthanum gallate crystal.

The color coordinates obtained by importing the emission data from the $\text{LaGaO}_3:\text{Tb}^{3+}$ and $\text{LaGaO}_3:(\text{Tb}^{3+},\text{Li}^+)$ phosphors into the color coordinate calculation software are also displayed in Fig. 7. The color coordinates of the $\text{LaGaO}_3:\text{Tb}^{3+}$ and $\text{LaGaO}_3:(\text{Tb}^{3+},0.01\text{Li}^+)$ phosphors are (0.3481, 0.4228) and (0.3513, 0.4751), respectively, which means that the

Li^+ doping has a significant effect on the color coordinate position and the color rendering. What is more, these color coordinates approach the green visible light region. In short, the $\text{LaGaO}_3:\text{Tb}^{3+}$ phosphors prepared in this study can be considered a class of luminescent materials with improved emission performance in the green light region when excited by ultraviolet or blue colored light.

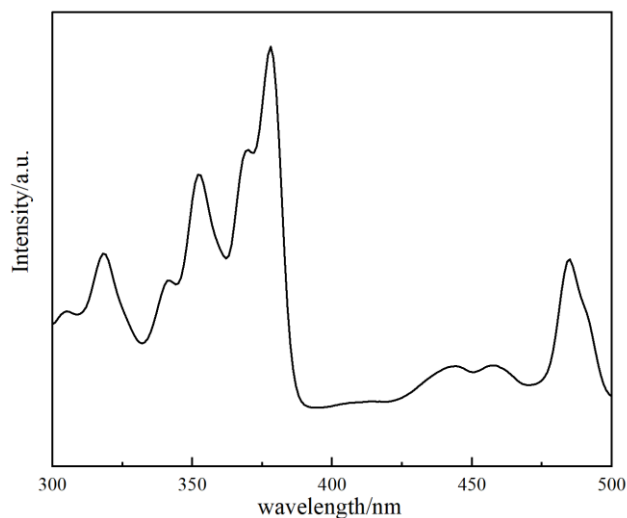


Fig. 5. Excitation spectrum of the $\text{LaGaO}_3:\text{Tb}^{3+}$ phosphor

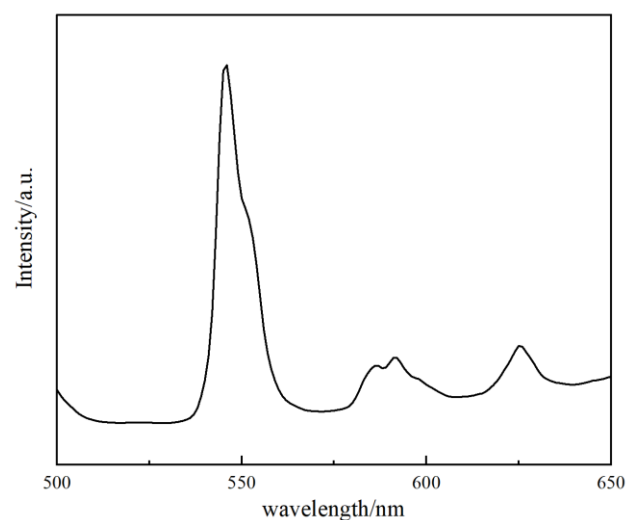


Fig. 6. Emission spectrum of the $\text{LaGaO}_3:\text{Tb}^{3+}$ phosphor

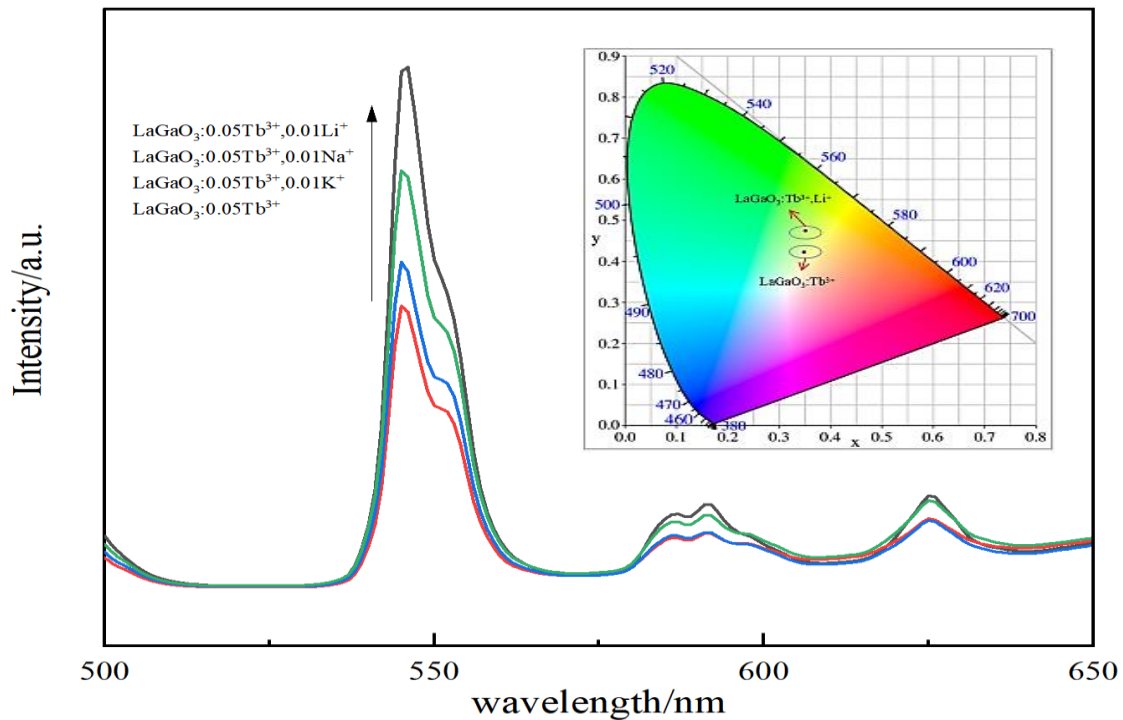


Fig. 7. Emission spectrum and color coordinates of the $\text{LaGaO}_3:(\text{Tb}^{3+}, \text{Li}^+/\text{Na}^+/\text{K}^+)$ phosphors (color online)

3.4. Luminescence mechanism analysis of $\text{LaGaO}_3:\text{Tb}^{3+}$ phosphors

The light decay curves of the samples were analyzed as well, and the lifetime with respect to Tb^{3+} was found to be 1.65 ms. The luminescence mechanism of the $\text{LaGaO}_3:\text{Tb}^{3+}$ phosphor powder is shown in Fig. 9. It can be seen that, after the Tb element is excited by ultraviolet light, its outer electrons undergo a $4f \rightarrow 5d$ energy level transition. The excited unstable high-energy state soon

returns to the lower-energy $4f$ level. In the $\text{LaGaO}_3:\text{Tb}^{3+}$ green phosphor, the ground-state spectral term of Tb^{3+} is given by 7F_4 state, while the excited states are $5d^1$, $5d^2$, $5d^3$, and $5d^4$ [10]. Because of the energy difference between the $4f$ and the $5d$ levels, the smallest variation is between the 7F_4 and $5d^1$ levels; therefore, this transition is most likely to occur within the Tb^{3+} transition process. The energy emitted by such a transition takes the form of a photon in the green visible light range.

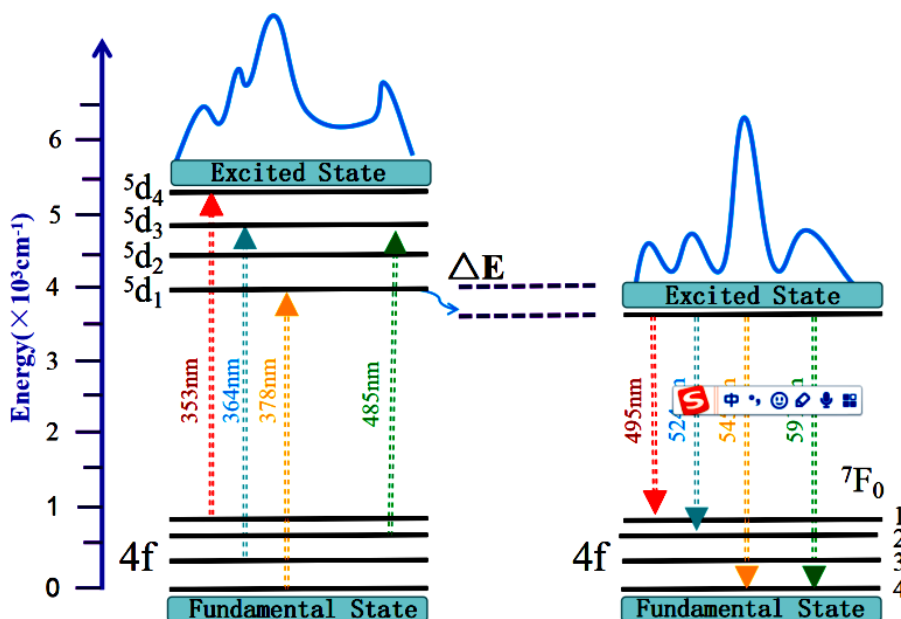


Fig. 9. Luminescence mechanism of the $\text{LaGaO}_3:\text{Tb}^{3+}$ phosphor (color online)

3.5. Analysis of a white LED device based on $\text{LaGaO}_3:\text{Tb}^{3+}$ phosphor

Commercial blue phosphors BAM and $(\text{Ca}, \text{Sr})\text{AlSiN}_3:\text{Eu}^{2+}$ red phosphors were added to the $\text{LaGaO}_3:\text{Tb}^{3+}$ green phosphors in a ratio of 7.5:2:1 for the green, blue, and red phosphors, respectively. A ZWL8820 organic gel was also used. The mass ratio of the silica powder was 1:1.2 for the mixing process. Fig. 9 depicts the spectrum from the white LED obtained under the

excitation of a 380 nm ultraviolet LED chip. The inset of Fig. 9 is a photograph of the LED after lighting. The color coordinates of the powder after the mixing of the three primary color phosphors are (0.3549, 0.3246), which are located in the white light regime. The CRI, CCT, and Color Purity values for the sample are respectively 89.5, 4471 K, and 86.3. This shows that $\text{LaGaO}_3:\text{Tb}^{3+}$ phosphors prepared in this study can be applied to the packaging of white LEDs.

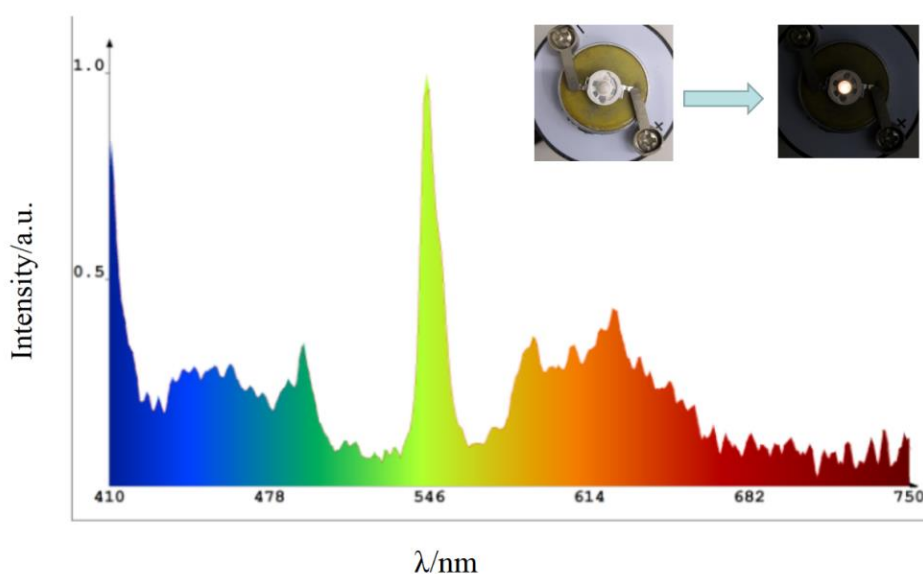


Fig. 9. Device spectrum of the $\text{LaGaO}_3:\text{Tb}^{3+}$ phosphor (color online)

4. Conclusion

The $\text{LaGaO}_3:\text{Tb}^{3+}$ green phosphors were obtained via high-temperature solid-phase calcination at a temperature of 1300 °C for 4 h. The incorporation of Tb^{3+} ions did not change the crystal phase structure of the matrix. The EDS results revealed that phosphors only contained a matrix doped with rare earth ions, which indicated the high purity of samples. The optimal excitation wavelength of the phosphors was 378 nm, while the strongest emission wavelength was 545 nm. The incorporation of Li^+ , Na^+ , or K^+ into the matrix did not alter the phase structure of the $\text{LaGaO}_3:\text{Tb}^{3+}$ phosphors, but it could effectively improve the luminescence properties of the latter ones. The color coordinates of the $\text{LaGaO}_3:\text{Tb}^{3+}$ phosphors were found to be (0.3481, 0.4228), which meant the ability of phosphors to emit relatively pure green visible light. This photoluminescence corresponds to the electronic transitions within the Tb^{3+} doping ions, which involve the 4f ground state and 5d excited state. Finally, using self-made phosphors as the raw materials and encapsulating them with commercially available red and blue phosphors, a white LED device with effective light emission was obtained.

Acknowledgements

This work was financially supported by Xi'an Science and Technology Committee Program (project no.GXYD9.2) and Shan'xi Educational Committee of the National Natural Science Foundation (project no. 17JK0395).

References

- [1] Zhiqiang Ming, Jing Zhao, Hendrik C. Swart, Zhiguo Xia, *Journal of Rare Earths* **38**(05), 64 (2020)
- [2] Zhigang Sun, Bin Lu, Guiping Ren, Hongbing Chen, *Nanomaterials* **10**(9), 1639 (2020)
- [3] Zhao Li, Kunyao Wu, Wang Yanan, Jing Cao, Yongfeng Wang, *Ferroelectrics* **582**(1), 63 (2021)
- [4] Zhao Li, Yongfeng Wang, Jing Cao, Yuanru Jiang, Xicheng Zhao, *Journal of Rare Earths* **34**(02), 143 (2016)
- [5] Abbi L. Mullins, Aleksandar Ciric, Ivana Zekovic, J. A. Gareth Williams, Miroslav D. Dramicanin,

- Ivana Radosavljevic Evans, Journal of Materials Chemistry C **10**(28), 10396 (2022)
- [6] S. Talari, S. K. Chirauri, P.V.S.S.S.N. Reddy, K. R. Rao, Materials Today Proceedings **52**, Part A, 2224 (2022).
- [7] Xiaoming Liu, Ran Pang, Zewei Quan, Jun Yang, Jun Lin, Journal of the Electrochemical Society **154**(7), J185 (2007)
- [8] Li Zhao, Wang Yong Feng, Cao Jing, Journal of Wuhan University of Technology (Materials Science) **33**(05), 1028 (2018).
- [9] Li Zhao, Zhao Xi-Cheng, Jiang Yuan-Ru, Journal of Rare Earths **33**(01), 39 (2015).
- [10] Xiaoming, Liu, Jun, Journal of Materials Chemistry **18**, 221 (2008).

*Corresponding author: pylizhao@163.com